Monthly Notices
of the
ROYAL ASTRONOMICAL SOCIETY

MNRAS **458,** 2953–2961 (2016) doi:10.1093/mnras/stw373
Advance Access publication 2016 February 16

Hydrogenation of CO-bearing species on grains: unexpected chemical desorption of CO

M. Minissale,★†‡ A. Moudens, S. Baouche, H. Chaabouni and F. Dulieu★

LERMA, Université de Cergy Pontoise, Sorbonne Universités, UPMC Univ. Paris 6, PSL Research University, Observatoire de Paris, UMR 8112 CNRS, 5 mail Gay Lussac, F-95000 Cergy Pontoise, France

Accepted 2016 February 12. Received 2016 February 12; in original form 2015 February 3

ABSTRACT

The amount of methanol in the gas phase and the CO depletion from the gas phase are still open problems in astrophysics. In this work, we investigate solid-state hydrogenation of CO-bearing species via H-exposure of carbon monoxide, formaldehyde, and methanol-thin films deposited on cold surfaces, paying attention to the possibility of a return to the gas phase. The products are probed via infrared spectroscopy (reflection absorption infrared spectroscopy), and two types of mass spectroscopy protocols: temperature-programmed desorption, and during-exposure desorption techniques. In the case of the [CO+H] reactive system, we have found that chemical desorption of CO is more efficient than H-addition reactions and HCO and H_2CO formation; the studies of the [H_2CO +H] reactive system show a strong competition between all surface processes, chemical desorption of H_2CO, H-addition (CH_3OH formation) and H-abstraction (CO formation); finally, [CH_3OH + H] seems to be a non-reactive system and chemical desorption of methanol is not efficient. CO-bearing species present a see-saw mechanism between CO and H_2CO balanced by the competition of H-addition and H_2-abstraction that enhances the CO chemical desorption. The chemical network leading to methanol has to be reconsidered. The methanol formation on the surface of interstellar dust grain is still possible through CO+H reaction; nevertheless, its consumption of adsorbed H atoms should be higher than previously expected.

Key words: astrochemistry – molecular data – molecular processes – methods: laboratory – ISM: molecules.

1 INTRODUCTION

Molecules, ubiquitous in space, provide powerful tools for probing the physics and chemistry of many different environments. CO has a unique role among molecules. The ^{12}CO (J=1→0) emission is commonly used to determine the total column density of molecular gas assuming a CO-to-H_2 conversion factor. Thus, CO is a popular tracer of remote Galaxy's dust-to-mass ratio (Bolatto, Wolfire & Leroy 2013).

Since the new measurements of the gas-phase ion-neutral chemistry leading to methanol by Geppert et al. (2006), the chemical models underestimated the methanol abundance in comparison with the observed abundances (Kristensen et al. 2010). In order to restore a good agreement with observed values, many models have included the possibility (Garrod, Wakelam & Herbst 2007; Vasyunin & Herbst 2013; Hocuk & Cazaux 2015; Ruaud et al. 2015; Cazaux et al. 2016) of the return into the gas phase thanks to the chemical desorption (hereafter CD). For example, Vasyunin & Herbst (2013) have demonstrated that methanol gas-phase abundance in several astrophysical environments can be explained by the desorption of a few per cent of methanol formed on the grain surfaces.

The fundamental difficulty of modelling the presence of complex organic molecules (COMs; e.g. Caselli & Ceccarelli 2012) in the gas phase in dark cloud environments (Bacmann et al. 2012) is due to their low formation rate in the gas phase compared to their accretion rates on solid surfaces. Therefore, even if COMs can form on the surface of dust grains (i.e. Butscher et al. 2015; Fedoseev et al. 2015) at a sufficient rate, there is a missing bridge between solid and gas phase where they are mostly observed thanks to their rotational spectra. In the reverse sense, the problem of selective depletion in pre-stellar cores has been known for many years (see review by Bergin & Tafalla 2007). In particular, Pagani, Bourgoin & Lique (2012), by studying N_2 and CO abundance in L183, have shown that CO presents a depletion of 300 higher than N_2 in the densest regions.

★ E-mail: marco.minissale@univ-amu.fr (MM); francois.dulieu@obspm.fr (FD)
† Present address: Aix Marseille Université, CNRS, PIIM UMR 7345, 13397 Marseille, France.
‡ Present address: Aix-Marseille Université, CNRS, Centrale Marseille, Institut Fresnel UMR 7249, 13013 Marseille, France.

To fully understand the initial conditions of star formation, one must consider solid-gas exchange which represents the main motivation for this paper. The case of CO and hydrogen reaction is particularly emblematic because historically it is the first system proposed with which to study desorption driven by chemistry (Takahashi & Williams 2000). In their work, Takahashi and Williams calculate the probability of CO desorption due to the local heating of the surface after formation of an H_2 molecule in its surrounding. This work illustrates from one side the inefficiency of indirect CD and from the other the need for a mechanism to return CO and CO-bearing molecules (HCO, H_2CO, CH_3O, CH_3OH) to the gas phase.

The understanding of the chemical networks leading to CO-bearing molecules is also crucial in planetary sciences since CO, H_2CO and CH_3OH are usually detected in comets (see review of Cochran et al. 2015). These species are believed to play a key role in the activity of these primitive bodies either as primary species or as COMs reaction products (Goesmann et al. 2015). CO is the molecule controlling the activity at large heliocentric distances of both long period and Jupiter family comets. CO can be a parent molecule originating from the nucleus of the comet or can also be produced as a daughter of H_2CO by photodissociation in the coma (Meier et al. 1993; Weaver et al. 2011; Le Roy et al. 2015). The observations of Comet 1P/Halley (Meier et al. 1993), 103P/Hartley 2 (Boissier et al. 2014), C/2012 F6 (Lemmon) and C/2012 S1 (Ison; Cordiner et al. 2014) showed that H_2CO can derive, in proportion of solar radiation flux, from sublimation, heating or photolysis in the coma of organic materials such as grains, polymers or other macromolecules. This hypothesis of H_2CO precursors will be ascertained by the COmetary Secondary Ion Mass Analyser (COSIMA) instrument on board of Rosetta spacecraft, analysing the dust grains emitted by the comet 67P/Churyumov-Gerasimenko.

The high abundance of CO-bearing species is well known also in interstellar ices as pointed out by many astronomical observations in the recent past (i.e. Whittet et al. 2011 and references therein). Total abundance of solid CO and hydrogenated CO-bearing species can vary from 15 per cent (of total ices) in molecular clouds towards field stars to 35 per cent for ices observed near low-mass young stellar objects. Due to these high abundances, a detailed knowledge of solid-state CO–H chemistry is mandatory in understanding the physical chemistry of the interstellar medium. For this reason, solid-state CO hydrogenation has been the subject of study by many theoretical (Goumans 2011; Rimola et al. 2014) and experimental groups (Hiraoka et al. 1994, 2002; Watanabe & Kouchi 2002; Watanabe et al. 2004; Fuchs et al. 2009; Pirim & Krim 2011).

CO hydrogenation can lead to formaldehyde and methanol formation through the following hydrogenation scheme, proposed very early in astrochemical models:

$$CO \xrightarrow{+H} HCO \xrightarrow{+H} H_2CO \quad R1a$$
$$H_2CO \xrightarrow{+H} CH_3O \xrightarrow{+H} CH_3OH \quad R2a$$

where in red we indicate undetected species (or hardly detected or subject to debate). Reactivity of CO+H is limited to *R1a* in Hiraoka et al. (2002), and continues to *R2a* in Watanabe et al. (2004) and Fuchs et al. (2009). Latter isotopic studies performed by Hidaka et al. (2009) have demonstrated that hydrogenation reactions can be followed by abstraction reactions leading to dehydrogenation of CO-bearing compounds, as for example the following reaction

$$CH_3OH \xrightarrow{+H} CH_3O + H_2 \xrightarrow{+H} H_2CO + 2\,H_2 \quad R2b \qquad (1)$$

Moreover, abstraction reactions are very important because they can lead to the deuteration of already formed species such like H_2CO and CH_3OH. By exposing D atoms to these molecules, it is possible to substitute the methyl group, but not the hydroxyl group.

At first sight, the results of experimental works about the hydrogenation of CO seem to lead to different conclusions. Watanabe & Kouchi (2002), Watanabe et al. (2004) and Fuchs et al. (2009) found that the [CO+H] reactive system leads to formaldehyde and methanol formation, while formaldehyde is the only species formed in Hiraoka et al. (1994, 2002). One of the main argument of these apparently diverging results is the difference in the fluxes (atoms per cm^2 per s) and fluences (total amount of atoms per cm^2) used in the experiments. Even if it is a secondary goal, our present investigation allows us to revisit again this fundamental divergence of the CO–H chemistry. We are aware that we use different experimental conditions and in particular we can explore sub-monolayer (ML) regime, using flux and fluences from 10 to 1000 lower than previous works. We have gathered the different experimental conditions and the main results/products of each works carried out so far in Table 1.

The unit of ML, is a surface density unit corresponding to 10^{15} particles cm^{-2}. It is convenient to use this unit because one can see directly if the substrate is thin or thick for the case of non-desorbing species, which is the case of hydrogen. H atoms are transformed promptly into H_2 which reaches a density steady state at 10 K of around few tenths of a layer (Dissly, Allen & Anicich 1994; Amiaud et al. 2007). Thus, the dose in ML for H indicates the maximum of reactions that can occur with it, and not the film thickness. For example, in our case, we sent only 6 ML of H atoms. If all the atoms would react with CO (<2.5 ML) molecules, the hydrogenation should not have been complete because CH_3OH requires at least four H atoms per CO molecule.

From Table 1, we can see that the experimental conditions are quite different, and therefore differences in observations are to be expected. Our present study focuses on low fluxes and fluences. Another important aspect is that the CO hydrogenation occurs only on the very first layers (see Fuchs et al. 2009 for a study of the effect of the CO thickness). The previous experiments do not really differ on this specific point since they all proceed with rather thick films. This prevents from studying thickness-dependent processes, i.e. CD. This last (also called reactive desorption) is the process which allows desorption in the gas phase of newly formed molecules on the surface. Our first experimental investigation of CD, carried on water formation system, shows a rather high efficiency (Dulieu et al. 2013). On the contrary, the following one based on oxygen reactivity (Minissale & Dulieu 2014), shows a very reduced efficiency of ozone CD (<4 per cent) and an important variation of O_2 CD with coverage and substrate. Therefore, the type and the thickness of the substrate is a parameter to be taken into account to study CD.

As clear from Table 1, the major differences of the experiments are fluence, flux and thickness. The effect of the fluence is easy to understand: up to the saturation point, the more H is sent, the more hydrogenation proceeds. The role of flux is more subtle to understand. The H-atom recombination rate on the surface increases as a function of H-atom flux and is the major chemical channel of the [CO+H] system. All H atoms will be used for CO hydrogenation only if each H atom is sent after the previous one has reacted with CO (and CO bearing species), because in this case, no H recombination is possible. Therefore, the lower the H flux, the higher the efficiency of hydrogenation (per H atoms). From Table 1, we can see that our experimental conditions should lead to the highest efficiency, even

Table 1. Some of the publications about the solid-state [CO+H] reactive system with experimental conditions and products.

Article	Flux (atoms×cm^{-2}s^{-1})	Fluence (atoms×cm^{-2})	(ML)	CO initial thickness (ML)	Major products of CO+H
Hiraoka et al. (2002)	10^{13}	3.6×10^{16}	36	≈10	H_2CO
Watanabe et al. (2004)	2×10^{15}	$>10^{17}$	<100	10	H_2CO and CH_3OH
Fuchs et al. (2009)	5×10^{13}	$>10^{17}$	<100	1–9	H_2CO and CH_3OH
This work	$\leq 2 \times 10^{12}$	$\leq 6 \times 10^{15}$	6	≤2.5	CO

if we stop the hydrogenation process very early. In our case, the total amount of H atoms sent on CO ices is two order of magnitude smaller with respect to Watanabe et al. (2004) and Fuchs et al. (2009). Our experimental conditions are somewhat similar to those of Hiraoka et al. (1994) and to date, the methanol production was almost non-detectable here starting from CO even by using both TPD technique and infrared (IR) spectroscopy.

This paper is organized as follows. The experimental set-up and methods are described in the next section. In Section 3, we present and discuss our experimental results on CO-bearing species hydrogenation. In the last section, we discuss the main conclusions and astrophysical implications of this study.

2 EXPERIMENTAL CONDITIONS

The experiments were conducted with the FORMOLISM (FORmation of MOLecules in the InterStellar Medium) set-up described in more details elsewhere (Amiaud et al. 2006; Congiu et al. 2012). It consists of an ultrahigh vacuum main chamber with a base pressure of 10^{-10}–10^{-11} mbar and two triply differentially pumped molecular or atomic lines. The ultrahigh vacuum chamber contains an oxidized slab of high-oriented pyrolytic graphite (HOPG, 0.9 cm in diameter), operating at temperatures between 8 and 400 K. The temperature is controlled by a calibrated silicon-diode sensor and a thermocouple (AuFe/Chromel K-type) clamped on the sample holder. Adsorbates and products are probed *in situ* through Fourier Transformreflection absorption infrared spectroscopy (FT-RAIRS) and a quadrupole mass spectrometer (QMS) used for measuring the beam flux and beam composition and for performing the temperature-programmed desorption (TPD) experiments. Moreover QMS is used to perform during exposure desorption (DED). In this case the QMS is placed in front of the sample in order to monitor the signal during the deposition phase. Through this method, we can probe desorption directly and study the CD (Dulieu et al. 2013; Minissale & Dulieu 2014; Minissale et al. 2016).

All the experiments are performed by performed by dosing different amounts of H atoms on to the CO (or H_2CO or CH_3OH) films previously grown on oxidized HOPG sample held at 10 K. The two species are deposited by using the same beam line at different times. After deposition, products are probed through RAIRS and TPD, using a thermal ramp of 10 K min^{-1} from 10 to 180 K.

Hydrogen atoms are generated by dissociating H_2 molecules in a quartz tube placed within a Surfatron cavity, which can deliver a maximum microwave power of 200 W at 2.45 GHz. With the microwave source turned on, the dissociation efficiency of H_2 was 30 ± 5 per cent at the sample.

We calibrated the molecular beam as described in Noble et al. (2011). The first ML (1 ML = 10^{15} molecules cm^{-2}) of CO, formaldehyde, and methanol were reached after an exposure time of 6, 12, and 15 min, respectively. The fluxes are the following: $\phi_{CO} = (3.0 \pm 0.3) \times 10^{12}$ molecules cm^{-2} s^{-1}, $\phi_{H_2CO} = (1.4 \pm 0.4) \times 10^{12}$ molecules cm^{-2} s^{-1}. The H-atom flux is $\phi_H = 2 \pm 0.7 \times 10^{12}$ atoms cm^{-2} s^{-1}.

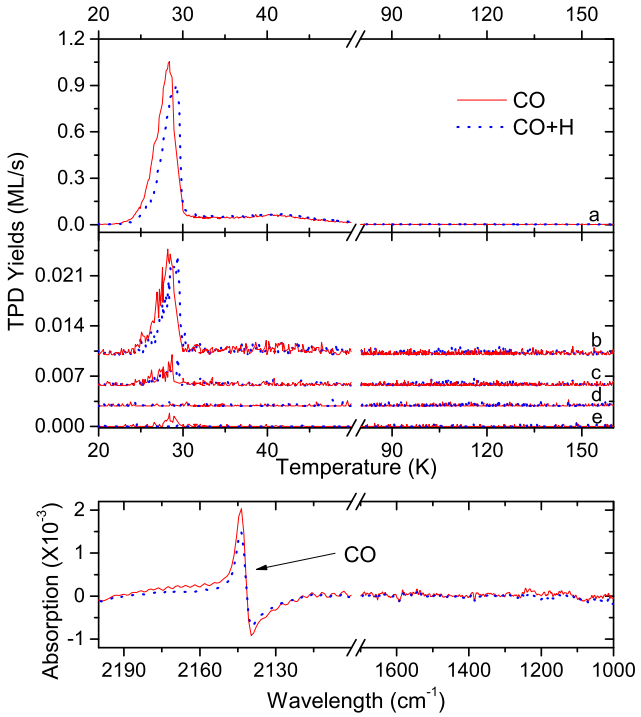

Figure 1. TPD traces (top panel) of mass 28, 29, 30, 31, and 32 m_u (*a*, *b*, *c*, *d*, and *e* curves respectively) and RAIRS spectra (bottom panel) after deposition of 2.5 ML of CO (red curves), and 2.5 ML of CO + 6 ML of H (blue curves) on oxidized HOPG held at 10 K.

3 EXPERIMENTAL RESULTS

In this section, we present the three different reactive systems [CO+H], [H_2CO+H], and [CH_3OH + H]. In all cases we have monitored all the possible products, ranging from CO to CH_3OH, via TPD and have recorded IR spectra. The DED results will be presented later.

3.1 TPD and RAIRS of the [CO+H] system

Fig. 1 shows the TPD curves of mass 28, 29, 30, 31, and 32 m_u and RAIRS spectra (bottom panel) after deposition of 2.5 ML of CO (red curves), and 2.5 ML of CO followed by 6 ML of H (blue curves) on oxidized graphite maintained at 10 K. For both depositions, the CO desorption profile of mass 28 appears as expected between 25 and 60 K. Similar peaks are also observed at mass 29 and 30. These two peaks are very probably due to the desorption of isotopes of carbon monoxide (^{13}CO and C^{18}O, respectively). We calculate the

ratio of areas under the peaks $^{13}CO/CO = 1.3$ per cent which is not far from 1.1 per cent found in IUPAC 1998. Similarly, the ratio $C^{18}O/CO = 0.3$ per cent fits exactly with what found by Hampel (1968).

The comparison between the two experiments (CO versus [CO+H]) suggests that only a small part of CO film has reacted with H atoms. Actually, the initial thickness is 2.5 ML at the end of the irradiation with 6 ML of H, 0.4 ML of CO is consumed (around 16 per cent of the initial ice coverage). Hiraoka et al. (2002), Watanabe et al. (2004) and Fuchs et al. (2009) have found a slower reactivity of CO with H atoms. For example, Fuchs et al. (2009) found that a fluence of H atoms of $\approx 2 \times 10^{16}$ cm^{-2} s^{-1} (i.e. 20 ML) is needed to consume 15 per cent of initial CO ice compared to 6×10^{15} cm^{-2} s^{-1} (i.e. 6 ML) to consume 16 per cent in our experiments.

More surprisingly, although we observe a measurable CO disappearance, we do not detect the expected H_2CO and CH_3OH products.

In our experiments, since neither H_2CO nor CH_3OH are detected (top panel in Fig. 1), we can estimate that *R1a* and *R2a* do not occur on the surface at measurable efficiencies. Very sensitive TPD spectra are confirmed by IR spectra in bottom panel of Fig. 1. We pinpoint that RAIRS results are used as an extra confirmation of TPD results; in this study, they do not provide any additional information on surface processes, since, especially on graphite surface, TPD is significantly more sensitive than RAIRS. The CO peak at 2140 cm^{-1} due to C–O stretching absorption bond decreases after the H-atom irradiation similarly to TPD curves, but we do not see any signature of formaldehyde nor methanol. We stress that the shape of IR absorption peak of carbon monoxide depends on the optical properties of graphite+CO system (surface thickness, polarization, and variation of complex refractive index of CO). Negative absorption between 2140 and 2120 cm^{-1} does not represent an effective emission of light by the system. It is due to a lower absorption of light (in this spectral range) of the graphite+CO system with respect to the case of bare graphite. In the case of CO adsorbed on water ice, CO presents a pure absorption peak (Palumbo & Strazzulla 1993).

We can sum up our experimental results with the [CO+H] system at low fluences and fluxes through the following statements.

(a) the reactivity of CO with H atoms is higher (more CO consumed, with the fluence being equal) with respect to that found in Watanabe et al. (2004) and Fuchs et al. (2009);

(b) the two products found by Watanabe et al. (2004) and Fuchs et al. (2009), namely formaldehyde and methanol, have not been detected;

(c) initial reactants > unreacted reactants + final products : something is lost.

3.2 TPD and RAIRS of the [H_2CO+H] system

The hydrogenation of H_2CO is richer and much more informative. Fig. 2 shows the TPD curves of mass 28, 29, 30, 31, and 32 m_u after deposition 1.8 ML of H_2CO (red curves), and 1.8 ML of H_2CO followed by 3.6 ML of H exposition (blue curves). Three main peaks are visible in the figure: between 25 and 60 K due to CO desorption; between 85 and 130 K due to H_2CO desorption; between 130 and 160 K due to CH_3OH desorption; each one of these peaks is detected via different masses depending on the cracking pattern of each molecule. We notice by comparing the TPD curves after 1.8 ML of H_2CO and 1.8 ML of H_2CO + 3.6 ML of H that a large

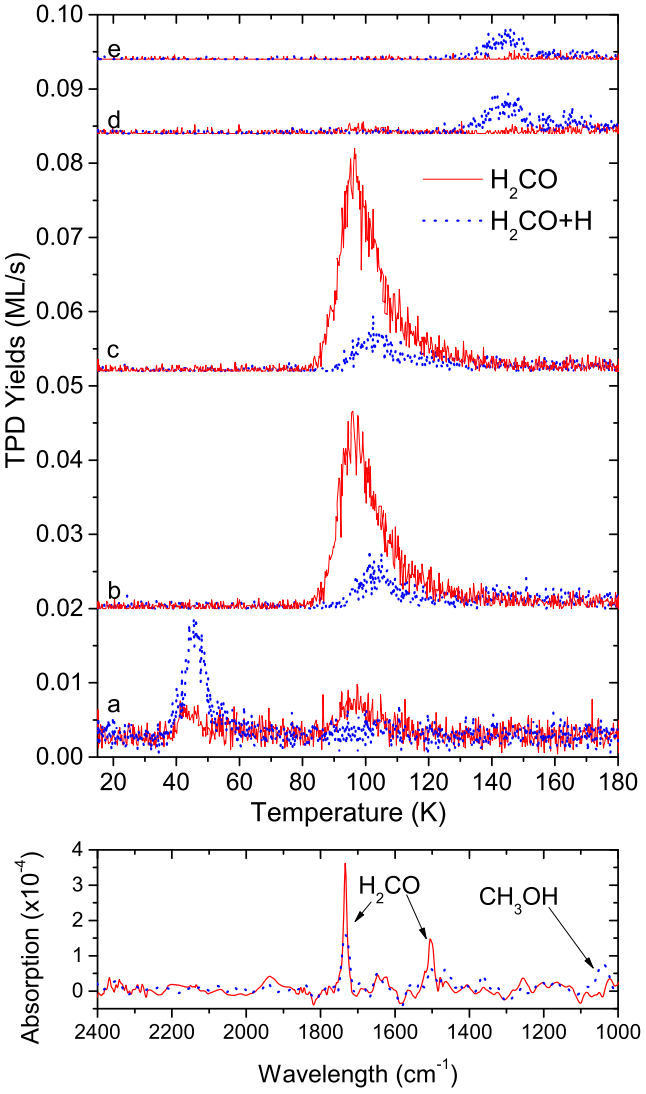

Figure 2. TPD traces (top panel) of mass 28, 29, 30, 31, and 32 m_u (*a*, *b*, *c*, *d*, and *e* curves, respectively) and RAIRS spectra (bottom panel) after deposition of 1.8 ML of H_2CO (red curves), and 1.8 ML of H_2CO + 3.6 ML of H (blue curves) on oxidized HOPG held at 10 K.

part of the formaldehyde is consumed: after H-atom irradiation, 1.4 ± 0.3 ML of initial formaldehyde ice is consumed and only 0.4 ± 0.2 ML remains unreacted. By looking at the CO and CH_3OH peaks, we estimated that 0.25 ± 0.2 ML of CO and 0.3 ± 0.1 ML of CH_3OH are formed. We can explain these products through the following hydrogenation scheme

$$H_2CO \xrightarrow{+H} HCO + H_2 \xrightarrow{+H} CO + 2\,H_2 \quad R1b$$
$$H_2CO \xrightarrow{+H} CH_3O \xrightarrow{+H} CH_3OH \quad R2a$$

although we cannot explain the lack of CO (under the form of CO, H_2CO, and CH_3OH molecules) at the end of the irradiation, like in the case of the [CO+H] experiment. We can sum up [H_2CO+H] experimental results through the following statements.

(d) the reactivity of H_2CO with H atoms is apparently more efficient than the [CO+H] reactivity;

(e) [H_2CO+H] leads to two products: CO and methanol;

(f) initial reactants > unreacted reactants + final products : something is lost.

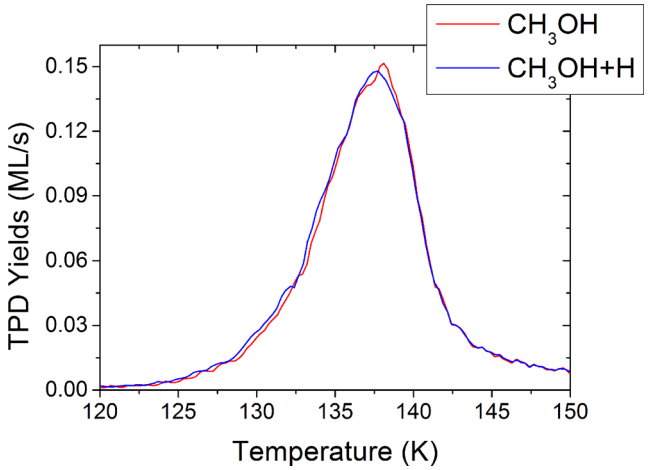

Figure 3. TPD traces (top panel) of mass 31 u.m.a after deposition of 1.2 ML of CH_3OH (red curves), and 1.2 ML of CH_3OH + 6 ML of H (blue dotted curves) on oxidized HOPG held at 10 K.

3.3 The [CH_3OH+H] system

Experiments were performed on oxidized graphite. Different CH_3OH ice thickness were irradiated with different doses of H. Fig. 3 exhibits the TPD spectra of mass 31 after a deposition of 1.2 ML of CH_3OH, followed or not by H exposition. Desorption profiles look exactly the same. We do not detect any measurable variations of the CH_3OH yield or any other newly formed species. The solid-state consumption routes for CH_3OH seems to be inefficient under our experimental conditions. If abstraction reactions occur, they are counterbalanced by hydrogenation reactions, but this time, no products are lost, contrarily to the case of [CO+H] experiments. We can summarize our finding on this system by one sentence.

(g) H-exposure of methanol has no measurable effects under our experimental conditions.

3.4 DED experiments

The DED technique consists in monitoring species in the gas phase during the deposition of the reactive species. Here, each possible masses (from 28 to 31), is monitored after the deposition of the CO bearing species, before and during the H exposure. The signals are very weak, and background signals (especially of mass 28) enlarge the error bars. In Fig. 4, the height of bars corresponds to the mean of the measured values (in ions counts per second), whereas the error bars show standard error of the measurements.

Fig. 4 shows the results of DED experiments for mass 28, 29, and 30 during exposure of H atoms on 2.5 ML of CO ice (α panel) and on 1.8 ML of H_2CO (β panel) on the graphite substrate held at 10 K.

For the mass 28, both [CO+H] and [H_2CO+H] experiments show an increase in the gas phase when H atoms are sent. However, it is more important for the [H_2CO+H] case, which is absolutely in line with the statement (d). CD of CO molecules after HCO+H-abstraction reaction should be the same for the [CO+H] and the [H_2CO+H] system, but the higher reaction rate in the [CO+H] system makes mass 28 DED signal larger. The differences in the signals are consistent with the different reaction rates deduced by TPD and RAIRS. Mass 28 could be also a cracking pattern of HCO,

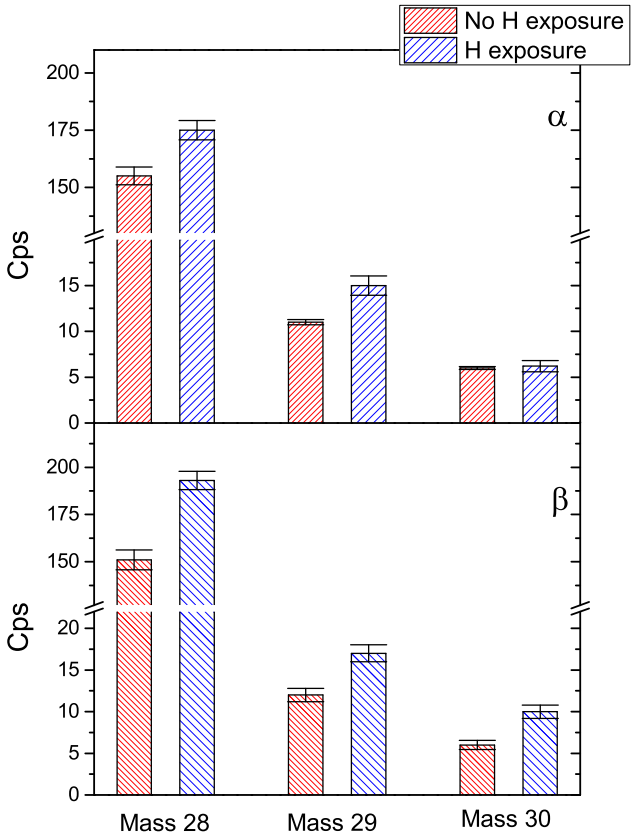

Figure 4. Integrated results of during exposure desorption (DED) experiments for mass 28, 29, and 30 before (red) and during (blue) H-irradiation of 2.5 ML of CO (α panel) and of 1.8 ML H_2CO (β panel) adsorbed on graphite held at 10 K.

but it is unlikely, taken into account the weakness of the mass 29 signal (parent molecular ion signal).

On the other hand, H_2CO is only positively detected in the [H_2CO+H] experiment. The absence of H_2CO in the case of [CO+H] can be correlated to the absence of H_2CO produced at the end of the experiments. At least this shows that the CD of H_2CO is not the reason of the lack of H_2CO as a final product in our experiment.

Mass 29 corresponds to HCO. It could be the cracking pattern of H_2CO (few per cent), but because mass 30 is very low, this is not the case. It could also be a contribution of ^{13}CO, but here again the difference is one order larger than expected for this isotopic contribution. The HCO signal is present in both experiments but is weaker by a factor of 2 at least than the CO signal. Note that raw signals cannot directly be compared quantitatively because the efficiency of detection is not the same for all the masses. However, this can still be taken as an indication that CO CD efficiency is larger than those of HCO.

An overview of CD is shown in Table 2, where we have considered DED of different masses, in CO/H_2CO+H experiments. From the present set of new experiments, we can add the following sentences.

(h) CD is responsible for the decrease of the CO bearing species.

(i) The CO CD is certainly more efficient than for other compounds.

Table 2. List of CD signal and efficiency for different masses in CO/H_2CO/CH_3OH+H experiments [see Minissale et al. (2016) for more details].

Experiment	Mass 28		Mass 29		Mass 30		Mass 31		Mass 32	
	CD signal-CD efficiency (per cent)									
CO+H	Strong	40 ± 20	Weak	10 ± 5	No	<5	No	<5	No	<5
H_2CO+H	Strong	40 ± 20	Weak	10 ± 5	Weak	10 ± 5	No	<5	No	<5
CH_3OH+H	No	<5	No	<5	No	<5	No	<5	No	<5

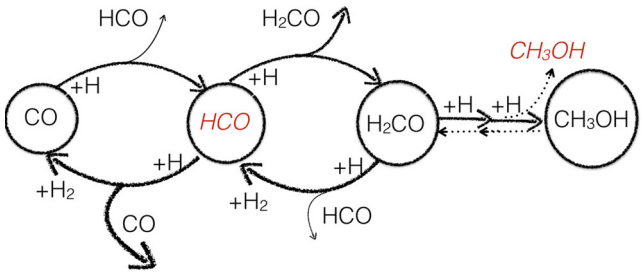

Figure 5. Scheme of the CO–H chemistry. The molecules in red are not detected in our experiments.

4 DISCUSSION

4.1 Diagram of reactions and processes

Even if sparsely disseminated in literature, the CO-bearing species and H network is known to be a competition between direct H-addition and H_2-abstraction of the methyl part. The experimental work of Hidaka et al. (2009) which summarizes many studies of this group clearly demonstrates the importance of the balance of the two processes, but did not include the first reverse step (HCO+H $\longrightarrow$ CO+H_2) which has not really been considered until now, except in the very recent work of Chuang et al. (2015). Not considering H_2-abstraction in competition with H-addition is a shortcut that can result in errors when implemented in astrochemical codes. One argument in favour of the competition of both mechanisms is that there is no clear gain in enthalpy of formation for the saturated species. At least, if we consider CO and H_2CO, both of these molecules have an enthalpy of formation of about 100 kJ per mole. Therefore, if we compare the two possible ends of the very exothermic HCO+H reaction, we easily conclude that CO+H_2 or H_2CO have about the same final total enthalpy, because by definition H_2 enthalpy of formation is equal to zero. However, this remark about the final energies tells nothing about the barriers to reaction, but only confirms that all the reverse reactions to hydrogenation should be included in the [CO+H] network without taking a risk. Moreover, statement (e) demonstrates that the HCO+H $\longrightarrow$ CO+H_2 route is effective. Because of the competition between addition and abstraction, the reactive system is probably looping between CO and HCO, and is probably also looping between HCO and H_2CO.

Fig. 5 shows the whole [CO+H] network leading from CO to CH_3OH and passing via the pivotal H_2CO molecule, and two radical molecules, undetectable in our experiments. HCO is explicitly represented, but we did not include CH_3O or CH_2OH, two possible radical intermediate isomers between H_2CO and CH_3OH. We exclude all other undetected species. We will discuss later this point. This diagram brings light on the fact that all species and especially CO, HCO and H_2CO are both adducts and products. It is obvious for the case of H_2CO, but it is less obvious for CO and CH_3OH that are at both ends of the chain. Taking into account the final products of the [H_2CO+H] experiments (almost the same amount of CO and CH_3OH), we can constraint the branching ratio of *R1b*/*R2a* to 50/50 (±25) per cent. However, the two branches are asymmetrical. The route to methanol seems to be one way, whereas the route to CO is certainly looping, or at least subject to both abstraction and addition. CH_3OH appears to be chemically stable, and seems to be not affected by H-addition [statement (g)], however, it has been shown that it can be deuterated, and that this should occur thanks to the abstraction mechanism (Hidaka et al. 2009). One possible explanation of absence of chemical activity observed in [CH_3OH+H] experiments can stand in the two possible isomers of the intermediate. The hydrogenation of H_2CO could lead to CH_3O, whereas CH_3OH+H $\longrightarrow$ CH_2OH+H_2. The two isomers CH_3O and CH_2OH reacting with H have possibly not the same branching ratio for H_2-abstraction and H-addition. Butscher et al. (2015) performed IR spectroscopy of photoinduced radicals as well as quantum calculations and demonstrated that CH_2OH is the favoured isomer to form CH_3OH. On the other hand, CH_3O has always been considered as the first step of H_2CO+H reaction. We can therefore propose that CH_3O may isomerize to CH_2OH thanks to its lower enthalpy of formation. This could happen via quantum tunnelling, or proton exchange with the ice environment. In our experimental conditions, due to the low flux of H, the average time between two reactions per adsorption site is rather long (about 300 s), and such a slow mechanism could be favoured. The net result would be that the CH_3O/CH_2OH steps does not allow the return of the CH_3OH to H_2CO, and that CH_3OH is only looping with CH_2OH.

Even if it is a raw extrapolation, the observation of the formation of glycolaldehyde and ethylene glycol by Fedoseev et al. (2015) and Chuang et al. (2015) from [CO+H] experiments becomes quite straight from our diagram. Actually HCO and CH_2OH concentration should be highly enhanced thanks to the loops, and therefore recombination products are likely to appear. In our experimental conditions, the two heavy molecules were not produced in measurable amounts, which is absolutely in line with our non-detection CH_3OH molecules, still the major compound (with H_2CO) formed in these previous experiments.

We can sum up our reaction network by considering three processes.

(i) Methanol is formed via H_2CO hydrogenation. It is the only inert and stable (in the sense that it cannot be consumed by H atoms) molecule in the CO–H chemistry; speculation: it could be a consequence of the two possible isomers of the intermediate species.

(ii) H_2CO can be both hydrogenated to form methanol or dehydrogenated to form CO. In the dehydrogenation process, CD can occur. Its efficiency is high (around 40 per cent).

(iii) CO can be hydrogenated to form formaldehyde but, even in this case, CD can occur, due to dehydrogenation reactions or due to H_2CO CD.

4.2 Comparison with previous experimental results on the [CO+H] system and substrate effects

Directly comparing experiments is a nonsense since fluence, flux, and substrate (CO ice thickness) are of importance. The detection

or non-detection of methanol in the [CO+H] experiments directly depends (at least) on these three parameters. The fluence helps the CH_3OH formation, but the flux also plays a central role because it displaces the chemical equilibrium in the case of reversible reactions. On one hand, the hydrogenation can occur by simple H-addition; but on the other, it is clear that the abstraction mechanism is a strong counter mechanism. Therefore, the final degree of hydrogenation is not only a question of fluence, but is, for a given flux, a chemical equilibrium between abstraction and addition in competition with the H+H reaction. Taking into account fluxes and fluences, we can conclude that all experimental results previously published are rather coherent. H-atom flux explains mostly the differences in CO consumption. Fluences and CO ice thickness explain mostly reactivity and final products obtained. Roughly the higher the fluence, the higher the probability for *R1a* and *R2a* to occur. This point is coherent with all experimental results; in fact we know that

$$\text{Fluence}_{\text{This work}} < \text{Fluence}_{\text{Hiraoka}} < \text{Fluence}_{\text{Fuchs and Watanabe}}$$

and the main products are, respectively, CO (this work), H_2CO (Hiraoka et al. 2002), H_2CO and CH_3OH (Watanabe et al. 2004; Fuchs et al. 2009). The apparent non-conservation of matter in our experiments (initial reactants> unreacted reactants + final products) can be explained through the third physical–chemical parameter, CO ice thickness. Watanabe et al. (2004) have performed their experiments for large CO ice thickness (120 Å > 10 ML), while Fuchs et al. (2009) have used variable CO ice thickness (from 1 to 10 ML) showing that the efficiency of H_2CO and CH_3OH formation increases as a function of CO ice thickness, up to a saturation limit obtain after few layers. The thickness (and/or the substrate) affects the reactivity and final degree of hydrogenation, for a given flux and fluence. We point out that we obtained the lowest degree of hydrogenation even if we had the highest reactivity. This is because of the CD pumping process. We stress that, in our flux conditions, the system cannot accumulate energy from the surface-absorbate complex, since time-scale for vibrational relaxation of adsorbates is significantly smaller than time-scale between reactive events. Vibrational relaxation time-scale goes in fact from some femtosecond in graphite, due to electron-hole pair relaxation, to some picosecond on silicates and Amorphous Solid Water (ASW) ice, thanks to adiabatic vibrational energy redistribution.

In our case of very thin layers, the substrate can play a role. It has been shown that the desorption dynamics after photoabsorption of UV photon was a surface indirect mechanism; i.e. the presence of water (a 'soft' layer) is able to quench the photodesorption process (Bertin et al. 2012). The local environment of the molecules plays a key role in the photodesorption efficiency, and it is the same for the CD. It is because we knew that the (photo)desorption of CO on a rigid substrate of less than 3 ML is not very reduced that we choose to perform our study with an oxidized graphite substrate. This can be a controversial choice, since no one can fully exclude that the substrate itself does not play a chemical role. We have arguments to think that the substrate is not chemically active, in the sense that it cannot exchange atoms with adsorbates. Physical properties (energy transfer, diffusion rates, adsorption sites density...) of different substrates influence only quantitatively chemical rates, whereas chemical activity of the substrate could change fully the reaction scheme. The absence of chemical activity of our substrate is supported by different points. First, no IR signature like C–H stretching bonds appeared during the experiments. Secondly, the coverage of molecules (in the < 3 ML limit) did not change qualitatively our observations, and experiments carried on other substrates (silicates and ASW ice) do exhibit the same trends. We performed another set of experiments, made directly on the cold golden mirror as a substrate and qualitatively confirmed the results of Fuchs et al. (2009) the thickness effects. Thus, we confirm that H-atoms penetration is not very efficient, and that atoms can hardly go through the films we deposited in the present experiments, and as such make the substrate poorly exposed to H reactivity. If our substrate is playing a chemical role, it is minor in the results we have shown here.

There is a possibility that the H+H reaction, which release more than 4 eV of energy, can locally heat the surface and promote desorption. Even if we cannot fully exclude this mechanism, we did not incorporate it in our scheme for different reasons. First, the loss of matter in [H_2CO+H] experiments is as high as in [CO+H] experiments; in the first case the probability of H+H reactions is smaller, and the number of CO available to indirect desorption is also lower. Secondly, we have performed complementary experiments with non-reactive species (i.e. [Ar+H] and [N_2+H]) without having any evidence of indirect desorption. For this reason, we have favoured a direct chemical action in our scheme.

Still, our experimental results appear to be extreme, in the sense that even no H_2CO have been detected on our oxidized graphite substrate in [CO+H] experiments. We have shown thanks to the DED measurements that it is due to CD. The CD is maximized on the graphite substrate and could be as high as 40 per cent for CO after the HCO+H reaction, even if, due to the possibility of few loops, it could be a reduced value. This high value of CD efficiency is the main reason of our choice of such a substrate, but other experiments carried on other substrates gave similar (although less extreme) results. Previous experiments performed on water ice substrate, and on silicate substrate showed exactly the same trends with the exception that H_2CO has been detected. This can be seen in the fig. 2 of Noble et al. (2012). We notice that the production of H_2CO was about twice efficient for the case of water substrate than for the case of silicate substrate, and we point out today that more than 50 per cent of the CO molecules also disappeared during the reaction phase. DED had not been performed at that time. The results obtained with H_2CO formation and CD are exactly in line with what we observed for the case of water formation (Dulieu et al. 2013). CD is lower on water ice substrate because of its ability to dissipate more efficiently the excess energy released during reactions. To be complete, water substrate is the only substrate where we could detect methanol after [CO+H] experiments, indicating again that the CD is a strong break to final hydrogenation of CO.

4.3 Astrophysical implications

The modification of the reaction network, including a very efficient abstraction mechanism has different implications. Up to now CO abundance in space was estimated via gas-phase reactions, photodissociation and sometimes subsequent accretion on dust grains (i.e. Glover & Low 2011; Pagani et al. 2012). Furthermore, it is known that solid-state reactions are at a certain degree able to consume CO (to form CO_2 or CH_3OH; i.e. Taquet, Ceccarelli & Kahane 2012), but no solid-state reactions able to form CO were known. Even if it is anecdotal, CO can also be formed directly in the solid state, by dehydrogenation of H_2CO.

One other effect of the modification of the reaction network is that H_2 can be formed at each advanced step of the hydrogenation of CO, thanks to the abstraction mechanism. The H_2 formation is known to occur on dust grains, that the observed values are basically

the balance between their destruction rates via UV photons and their formation of the grains (Habart et al. 2005). Actually, the H_2-abstraction of HCO should not change the H_2 formation, since it is a sub-category of physisorbed processes. The efficiency of the physisorbed processes is a balance between desorption and diffusion, and its main efficiency limit is due to the temperature of the grain (Bron, Le Bourlot & Le Petit 2014). Even if some CO molecules could be present at a temperature as high as 30 K (Noble, Diana & Dulieu 2015), H_2CO, formed in gas phase and later accreted even at higher temperatures (Noble et al. 2012), may be a catalyst intermediate to H_2 formation, but again it should be a minor route. Even if we demonstrated that we can consider the hydrogenated CO bearing molecules as H_2 catalysts, the presence of all the steps of the catalysis is mandatory, and therefore is limited by the rather low binding energy of CO. For environments where the surface of grains is at higher temperature, the abstraction mechanism can be an efficient process to catalysis, but polycyclic aromatic hydrocarbon are probably better catalytic substrates than CO bearing species (Boschman et al. 2012; Thrower et al. 2012).

If H_2 formation should not really been affected by the modification of the reaction network, methanol formation should be impacted. The main effect should be a slower rate of formation, or at least, a larger H consumption to obtain a full hydrogenation of CO. The cycling steps should delay the CH_3OH production. The CO CD, could be compensated by a CO accretion, and should not be a total break like it can be in our experiments, especially when an ice sub-layer is present. However, if the time to transform CO to methanol increases, and if each step has to be crossed more often, the probability of diverging from the only hydrogenation processes increase. Especially, H_2CO is known to react with O to form CO_2 (Minissale et al. 2015), therefore the final balance CO_2 to CH_3OH should be modified in favour of CO_2. As pointed out by Chuang et al. (2015), another possible issue for the hydrogenation of CO is glycoaldehyde and related compounds.

Finally, incorporating a balance between abstraction and H-addition, should change the way that effective barriers for the CO hydrogenation have been derived. Barriers (total or entrance) should be lower than previously estimated. However, the derivation of such barriers is beyond the scope of this article and requires long studies implying, for example, the possibility of changing the fluxes, which is not yet possible in our present set-up.

The main finding of our study is that adsorbed CO can go back into the gas phase, even from cold grains ($<$15 K), under the action of two successive H atoms. It is not clear if this mechanism can affect the CO snowline as for example observed in episodic accretion events (Visser, Bergin & Jørgensen 2015) during low-mass star formation. At most, the return to the gas phase involves about one CO molecule over two. Reducing by a factor of 2, the effective accretion rate can induce some shifts, but the macroscopic dynamical processes should stay dominant. When thermal desorption is at play, a factor of 2 is balanced by a small difference in the grains temperature. For quieter environments, where the temperature of grains is less than 15 K, the CD of CO and CO bearing species can delay the depletion, and should be able to sustain a fraction of CO, in the gas phase. It is not what is observed in the very centre of pre-stellar cores, where depletion can be very high, up to $CO/H_2 = 6.6\ 10^{-8}$ (Pagani et al. 2012). However, the abundance in the gas phase of a species is a complex product of the physical and chemical history of a media, and a low value of CO in the gas phase can also means that the CO to COMs chemical journey is well advanced, and that less CO is available at the very surface of interstellar dust grains.

4.4 Concluding remarks

The hydrogenation of CO is one cornerstone of solid-state astrochemistry. We have shown that the direct hydrogenation of CO to methanol is a too simple description of the chemical network. The hydrogenation of CO is probably better described by taking account the chemical equilibrium between H-addition and H_2-abstraction. Therefore, experimental conditions and especially the flux, change the balance of final products. On rigid surface, with low CO coverages, the CD is important and has two main effects. In experiments, it strongly inhibits the hydrogenation of CO. In space, it should slow the CO depletion, and delay its hydrogenation to methanol.

ACKNOWLEDGEMENTS

We acknowledge the support of the French National PCMI programme funded by the CNRS and the support of the DIM ACAV, a funding program of the Région Ile de France. MM thanks G. Baratta for fruitful discussions about results interpretation. CH_3OH is a target molecule of SOLIS, a NOEMA key program (PI: Caselli & Ceccarelli), and this work is part of its scientific purposes. We thank anonymous referee for his constructive review of our paper.

REFERENCES

Amiaud L., Fillion J. H., Baouche S., Dulieu F., Momeni A., Lemaire J. L., 2006, J. Chem. Phys., 124
Amiaud L., Dulieu F., Fillion J.-H., Momeni A., Lemaire J. L., 2007, J. Chem. Phys., 127, 144709
Bacmann A., Taquet V., Faure A., Kahane C., Ceccarelli C., 2012, A&A, 541, L12
Bergin E. A., Tafalla M., 2007, ARA&A, 45, 339
Bertin M. et al., 2012, Phys. Chem. Chem. Phys., 14, 9929
Boissier J. et al., 2014, Icarus, 228, 197
Bolatto A. D., Wolfire M., Leroy A. K., 2013, ARA&A, 51, 207
Boschman L., Reitsma G., Cazaux S., Schlathölter T., Hoekstra R., Spaans M., González-Magaña O., 2012, ApJ, 761, L33
Bron E., Le Bourlot J., Le Petit F., 2014, A&A, 569, A100
Butscher T., Duvernay F., Theule P., Danger G., Carissan Y., Hagebaum-Reignier D., Chiavassa T., 2015, MNRAS, 453, 1587
Caselli P., Ceccarelli C., 2012, A&AR, 20, 56
Cazaux S., Minissale M., Dulieu F., Hocuk S., 2016, A&A, 585, A55
Chuang K.-J., Fedoseev G., Ioppolo S., van Dishoeck E. F., Linnartz H., 2015, MNRAS, 455, 1702
Cochran A. et al., 2015, Space Sci. Rev., 197, 9
Congiu E., Chaabouni H., Laffon C., Parent P., Baouche S., Dulieu F., 2012, J. Chem. Phys., 137, 054713
Hampel C. A., 1968, The Encyclopedia of the Chemical Elements. Reinhold Book Corporation, New York, p. 499
Cordiner M. et al., 2014, ApJ, 792, L2
Dissly R. W., Allen M., Anicich V. G., 1994, ApJ, 435, 685
Dulieu F., Congiu E., Noble J., Baouche S., Chaabouni H., Moudens A., Minissale M., Cazaux S., 2013, Sci. Rep., 3, 1338
Fedoseev G., Cuppen H. M., Ioppolo S., Lamberts T., Linnartz H., 2015, MNRAS, 448, 1288
Fuchs G. W., Cuppen H. M., Ioppolo S., Romanzin C., Bisschop S. E., Andersson S., van Dishoeck E. F., Linnartz H., 2009, A&A, 505, 629
Garrod R. T., Wakelam V., Herbst E., 2007, A&A, 467, 1103
Geppert W. D. et al., 2006, Faraday Discuss., 133, 177
Glover S. C. O., Low M.-M. M., 2011, MNRAS, 412, 337
Goesmann F. et al., 2015, Science, 349, 6247
Goumans T. P. M., 2011, MNRAS, 413, 2615
Habart E., Walmsley M., Verstraete L., Cazaux S., Maiolino R., Cox P., Boulanger F., Des Forêts G. P., 2005, Space Sci. Rev., 119, 71
Hidaka H., Watanabe M., Kouchi A., Watanabe N., 2009, ApJ, 702, 291

Hiraoka K., Ohashi N., Kihara Y., Yamamoto K., Sato T., Yamashita A., 1994, Chem. Phys. Lett., 229, 408
Hiraoka K., Sato T., Sato S., Sogoshi N., Yokoyama T., Takashima H., Kitagawa S., 2002, ApJ, 577, 265
Hocuk S., Cazaux S., 2015, A&A, 576, A49
Kristensen L. E., van Dishoeck E. F., van Kempen T. A., Cuppen H. M., Brinch C., Jørgensen J. K., Hogerheijde M. R., 2010, A&A, 516, A57
Le Roy L. et al., 2015, A&A, 583, A1
Meier R., Eberhardt P., Krankowsky D., Hodges R., 1993, A&A, 277, 677
Minissale M., Dulieu F., 2014, J. Chem. Phys., 141, 014304
Minissale M., Loison J.-C., Baouche S., Chaabouni H., Congiu E., Dulieu F., 2015, A&A, 577, A2
Minissale M., Dulieu F., Hocuk S., Cazaux S., 2016, A&A, 585, A24
Noble J. A., Dulieu F., Congiu E., Fraser H. J., 2011, ApJ, 735, 121
Noble J. A., Congiu E., Dulieu F., Fraser H. J., 2012, MNRAS, 421, 768
Noble J. A., Diana S., Dulieu F., 2015, MNRAS, 454, 2636
Pagani L., Bourgoin A., Lique F., 2012, A&A, 548, L4
Palumbo M., Strazzulla G., 1993, A&A, 269, 568
Pirim C., Krim L., 2011, Chem. Phys., 380, 67
Rimola A., Taquet V., Ugliengo P., Balucani N., Ceccarelli C., 2014, A&A, 572, A70
Ruaud M., Loison J. C., Hickson K. M., Gratier P., Hersant F., Wakelam V., 2015, MNRAS, 447, 4004
Takahashi J., Williams D. A., 2000, MNRAS, 314, 273
Taquet V., Ceccarelli C., Kahane C., 2012, A&A, 538, A42
Thrower J. D. et al., 2012, ApJ, 752, 3
Vasyunin A. I., Herbst E., 2013, ApJ, 769, 34
Visser R., Bergin E. A., Jørgensen J. K., 2015, A&A, 577, A102
Watanabe N., Kouchi A., 2002, ApJ, 571, L173
Watanabe N., Nagaoka A., Shiraki T., Kouchi A., 2004, ApJ, 616, 638
Weaver H., Feldman P., A'Hearn M., Dello Russo N., Stern S., 2011, ApJ, 734, L5
Whittet D. C. B., Cook A. M., Herbst E., Chiar J. E., Shenoy S. S., 2011, ApJ, 742, 28

This paper has been typeset from a TEX/LATEX file prepared by the author.